Supplemental Figure 1, related to Figure 1

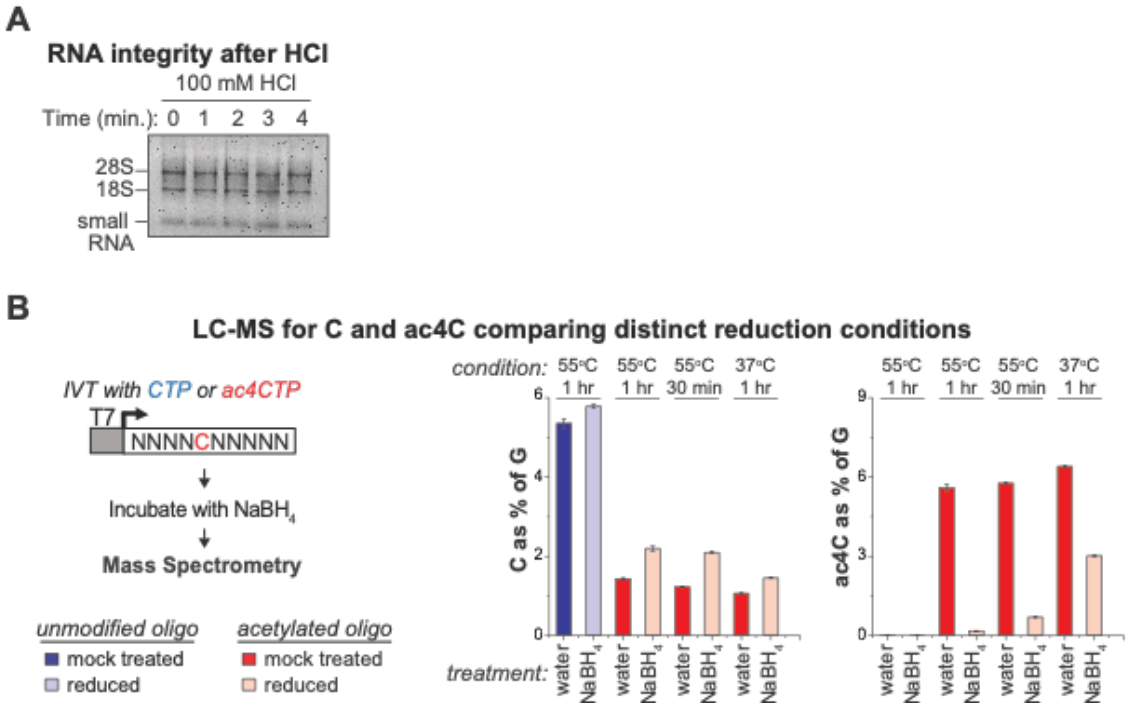

Figure S1. Optimization of reaction conditions used to chemically reduce ac4C. (A) Agarose gel analysis of total RNA integrity after exposure to the concentration of HCl used in $NaCNBH_3$ reduction (100 mM) for the indicated times. **(B)** Mass spectrometric analysis of C and ac4C levels in an RNA oligo containing a single ac4C after reduction with $NaBH_4$ under the specified reaction conditions. An unmodified RNA oligo with a single C serves as control. Data represent the Mean ± SD as a percent of detected guanosine, $n = 3$.

Supplemental Figure 2, related to Figure 2

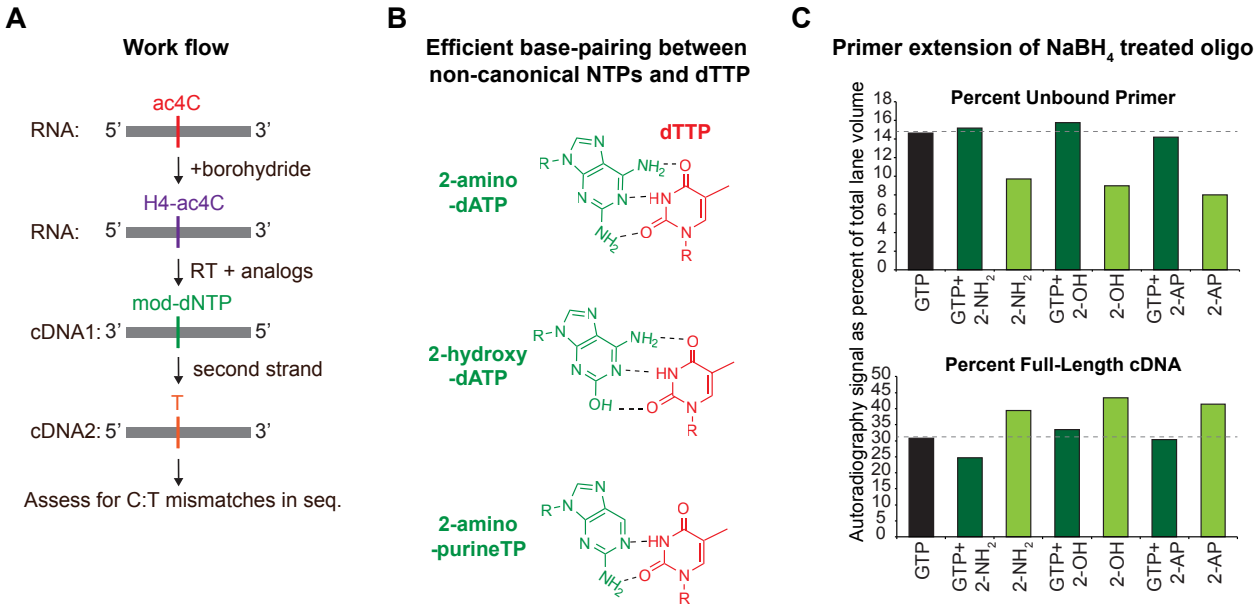

Figure S2. Non-canonical NTPs with base-pairing features that complement tetrahydro-ac4C improve cDNA synthesis through reduced ac4C. (A) Workflow schematic. **(B)** Base-pairing predictions support robust binding between non-canonical NTPs and dTTP during second strand cDNA synthesis. **(C)** Quantification of the primer extension results from $NaBH_4$-treated RNA from Figure 2D comparing the signal intensity associated with unincorporated primer or full-length cDNA as a percent of total lane volume. Volumes were derived from identically sized boxes in ImageQuant. 2-NH_2 = 2-amino-dATP; 2-OH = 2-hydroxy-dATP; 2-AP = 2-aminopurineTP.

Supplemental Figure 3, related to Figure 3

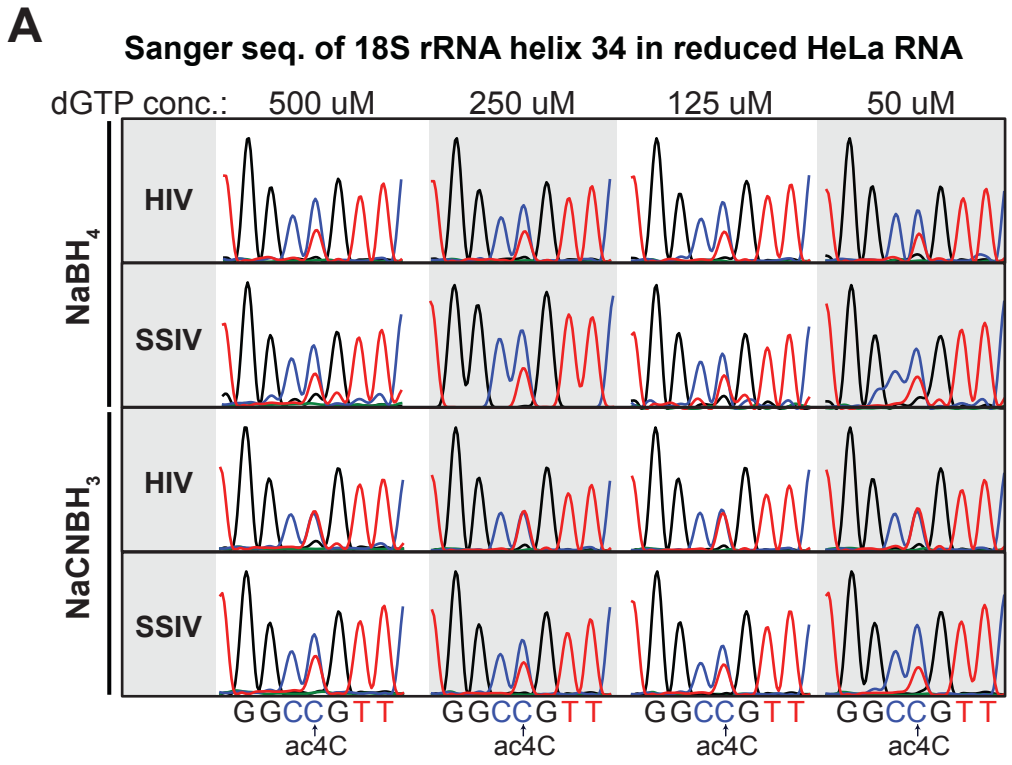

Figure S3. Limiting dGTP in cDNA synthesis is insufficient to reach high C:T mismatch levels at reduced ac4C sites. (A) Sanger sequencing traces of RT-PCR amplicons surrounding the ac4C site in 18S rRNA helix 34 from $NaBH_4$ and $NaCNBH_3$ reduced HeLa RNA reverse transcribed with HIV and SSIV RTases and decreasing concentrations of dGTP, corresponding to Figure 3C.

Supplemental Figure 4, related to Figure 4

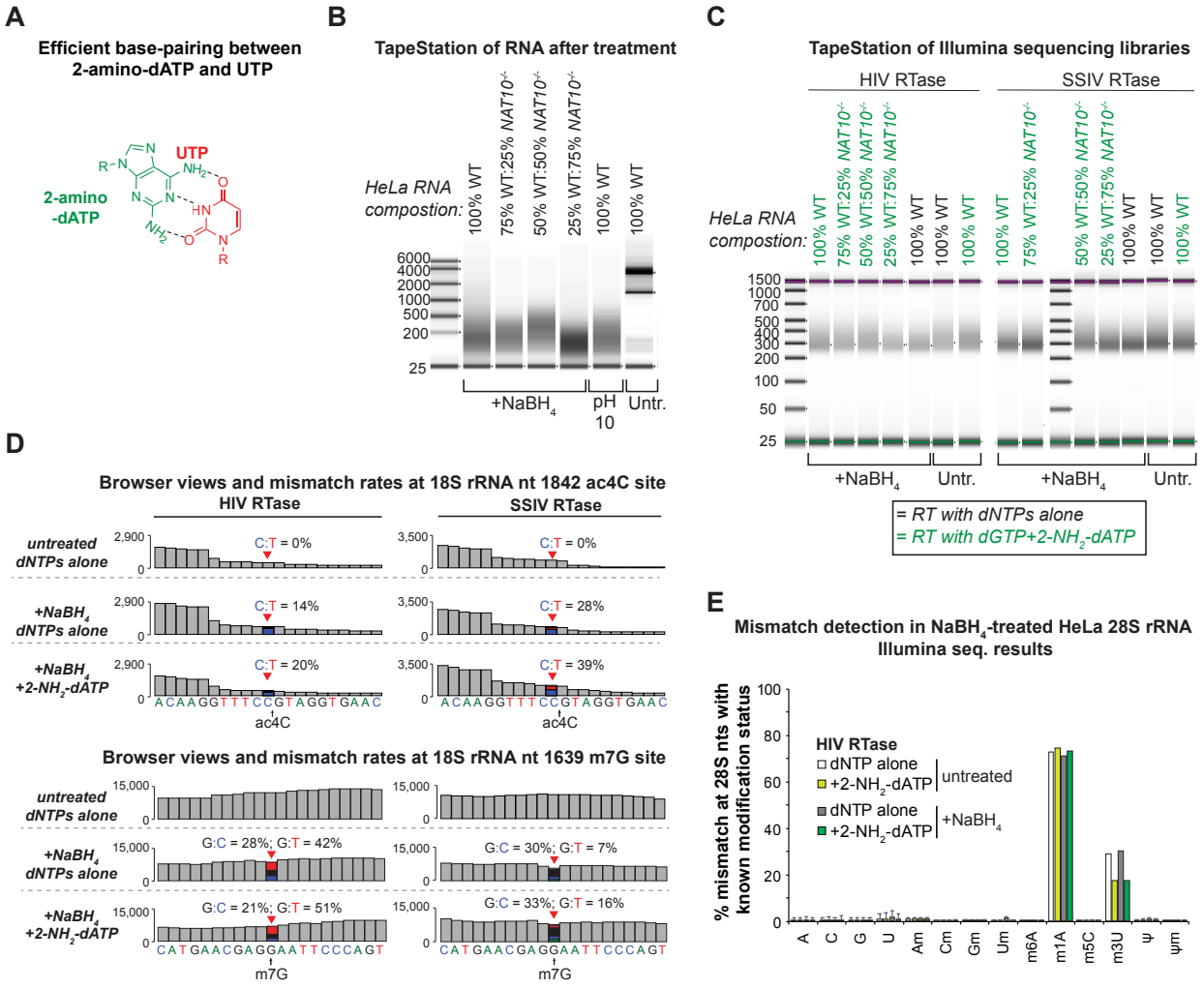

Figure S4. Assessing the specificity of RetraC:T for ac4C through Illumina sequencing. (A) Scheme depicting the base-pairing properties between 2-amino-dATP and UTP. The unnatural nucleotide can form three hydrogen bonds and be incorporated opposite of U in first strand cDNA synthesis. **(B)** Agilent Tapestation analysis after exposure of wildtype and *NAT10-/-* RNA in mixtures, as indicated, to $NaBH_4$-treatment or pH-matched control. Untreated (untr.) wildtype HeLa RNA is shown for comparison. **(C)** Agilent Tapestation analysis of cDNA libraries generated from the RNA in (B) through a custom reverse transcription pipeline with either HIV or SSIV RTases in the presence of the canonical dNTPs (black) or a mixture in which the dGTP component has been replaced with 25% dGTP:75% 2-NH_2-dATP (green). Untreated indicates pH-matched control. Library preparation was achieved through the NEBNext Ultra II Directional RNA library for Illumina kit. **(D)** Browser views surrounding the ac4C site at 18S nt 1842 and the m7G site at 18S nt 1639 from sequencing of untreated or $NaBH_4$-treated RNA reverse transcribed in the presence of 2-amino-dATP or dNTPs alone, as shown. C:T mismatches are depicted in red. **(E)** Cumulative mismatch rates from sequencing of untreated or $NaBH_4$-treated RNA reverse transcribed in the presence of 2-amino-dATP or dNTPs alone, derived from each of the 5064 nts in 28S rRNA and segregated by modification status.

Supplemental Figure 5, related to Figure 5

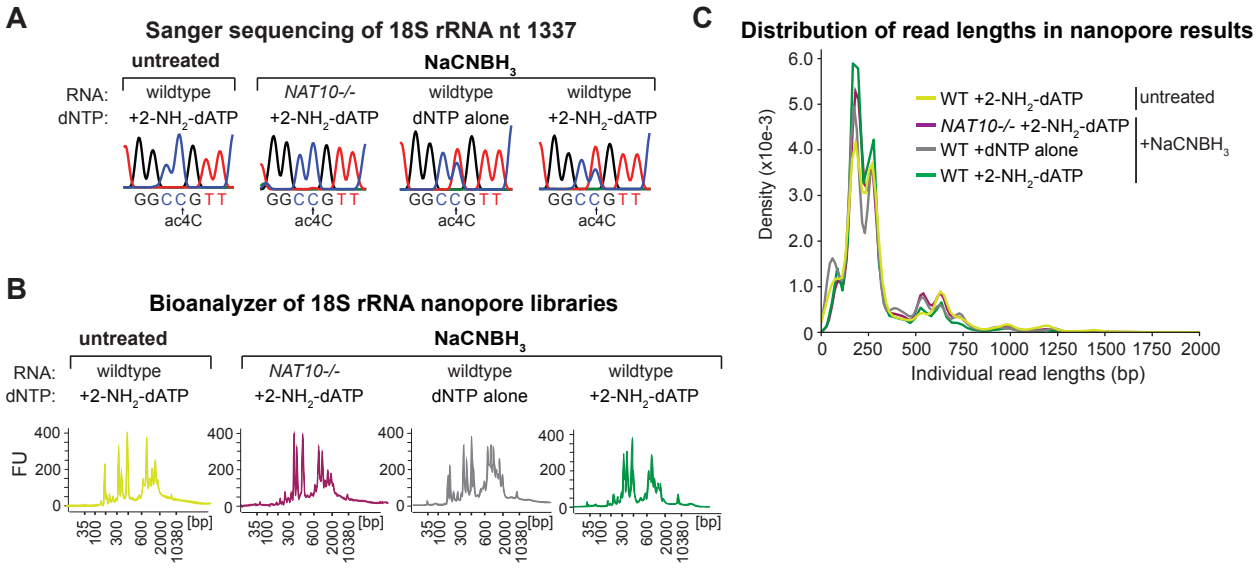

Figure S5. Assessing the specificity of RetraC:T for ac4C through nanopore sequencing. (A) Sanger sequencing traces surrounding the 18S rRNA helix 34 ac4C site at nt 1337 after $NaCNBH_3$ reduction of wildtype and *NAT10-/-* HeLa RNA and reverse-transcription with HIV RTase +/- 2-amino-dATP, as shown. **(B)** High sensitivity DNA bioanalyzer analysis of Nanopore-PCR libraries of purified 18S PCR products generated from the RT reactions from (A). **(C)** Distribution of read lengths from nanopore sequencing of 18S rRNA libraries from (B).